SIAM J. SCI. COMPUT.
Vol. 29, No. 1, pp. 245–264


# NUMERICAL METHODS FOR SECOND-ORDER STOCHASTIC DIFFERENTIAL EQUATIONS*

KEVIN BURRAGE†, IAN LENANE†, AND GRANT LYTHE‡

**Abstract.** We seek numerical methods for second-order stochastic differential equations that reproduce the stationary density accurately for all values of damping. A complete analysis is possible for scalar linear second-order equations (damped harmonic oscillators with additive noise), where the statistics are Gaussian and can be calculated exactly in the continuous-time and discrete-time cases. A matrix equation is given for the stationary variances and correlation for methods using one Gaussian random variable per timestep. The only Runge–Kutta method with a nonsingular tableau matrix that gives the exact steady state density for all values of damping is the implicit midpoint rule. Numerical experiments, comparing the implicit midpoint rule with Heun and leapfrog methods on nonlinear equations with additive or multiplicative noise, produce behavior similar to the linear case.

**Key words.** damped harmonic oscillators with noise, stationary distribution, stochastic Runge–Kutta methods, implicit midpoint rule, multiplicative noise

**AMS subject classifications.** 60-08, 65C30

**DOI.** 10.1137/050646032

## 1. Introduction.

Newton's second law of motion relates force to acceleration. Consequently, second-order differential equations are common in scientific applications, in the guise of "Langevin," "Monte Carlo," "molecular," or "dissipative particle" dynamics [1, 2, 3], and the study of methods for second-order ordinary differential equations is one of the most mature branches of numerical analysis [4]. The most exciting advances in recent decades have been the development of symplectic methods, capable of exactly preserving an energy-like quantity over very long times [5], and their extension to stochastic systems [6]. In the stochastic setting, the long-time dynamics of a typical physical system is governed by fluctuation-dissipation, so that the amount of time spent in different regions of phase space can be calculated from the stationary density [7]. This density can have a relatively simple explicit expression even when the dynamics is highly nonlinear [8]. Numerical methods replace continuous-time with discrete-time dynamics, generating values at times $t_0, t_1, \ldots$. Usually $t_{n+1} - t_n$ is a fixed number $\Delta t$. The criterion for a good numerical method that will be examined in this work is that its discrete-time dynamics has a stationary density as close as possible to that of the continuous-time system.

The differential equations describing second-order systems contain a parameter known as damping. The stationary density is independent of damping, but dynamical quantities, and the usefulness of numerical algorithms, are strongly dependent on it. In the infinite-damping limit, the system becomes first order. The limit of zero damping, on the other hand, corresponds to Hamiltonian systems, where symplectic methods can be applied. The aim in this paper is to devise methods capable of accurately reproducing the stationary density *for all positive values of damping.*

*Received by the editors November 24, 2005; accepted for publication (in revised form) August 10, 2006; published electronically February 2, 2007.
http://www.siam.org/journals/sisc/29-1/64603.html

†Advanced Computational Modelling Centre, Department of Mathematics, University of Queensland, Queensland 4072, Australia (kb@maths.uq.edu.au, ijl@maths.uq.edu.au).

‡Department of Applied Mathematics, University of Leeds, Leeds LS2 9JT, England (grant@maths.leeds.ac.uk).

We shall consider equations of the following form:

$$\ddot{x} = f(x) - \eta s^2(x)\dot{x} + \epsilon s(x)\xi(t), \tag{1.1}$$

where $\langle \xi(t)\xi(t') \rangle = \delta(t-t')$ and the damping parameter is denoted $\eta$. Angled brackets denote mean over realizations. The second-order stochastic differential equation (SDE) (1.1) describes the position of a particle subject to deterministic forcing $f(x)$ and random forcing $\xi(t)$. The deterministic forcing is related to the potential function $V(x)$ via $f(x) = -V'(x)$. The amplitude of the random forcing, $\epsilon$, is related to the temperature $T$ and damping coefficient $\eta$ by the fluctuation-dissipation relation [8] $\epsilon^2 = 2\eta KT$.

We can write (1.1) as a pair of first-order equations for $\mathbf{X}_t$ and $\mathbf{V}_t$, the position and velocity variables:

$$\begin{aligned} \mathrm{d}\mathbf{X}_t &= \mathbf{V}_t \mathrm{d}t, \\ \mathrm{d}\mathbf{V}_t &= -\eta s^2(\mathbf{X}_t)\mathbf{V}_t \mathrm{d}t + f(\mathbf{X}_t)\mathrm{d}t + \epsilon s(\mathbf{X}_t)\mathrm{d}\mathbf{W}_t, \end{aligned} \tag{1.2}$$

where $\mathbf{W}_t$ is a Wiener process satisfying $\langle \mathbf{W}_t \mathbf{W}_s \rangle = \min(t,s)$. If $s(x)$ is not a constant, the noise amplitude is a function of position and the equation is commonly said to have "multiplicative noise." However, because the coefficient of $\mathrm{d}\mathbf{W}_t$ in the SDE for $\mathbf{V}_t$ is a function of $\mathbf{X}_t$ only, there is no difference between the Ito and Stratonovich (see Gardiner [8]) forms of (1.2). The probability density at time $t$ is $P(x,v;t)$, where

$$P(x,v;t) = \frac{\mathrm{d}}{\mathrm{d}x}\frac{\mathrm{d}}{\mathrm{d}v}\mathrm{Prob}\left(\mathbf{X}_t < x, \mathbf{V}_t < v\right). \tag{1.3}$$

The stationary density, $P_\infty(x,v)$, defined as

$$P_\infty(x,v) = \lim_{t\to\infty} P(x,v;t), \tag{1.4}$$

has the following analytical form, independent of $\eta$ and $s(x)$ as long as $\eta > 0$ and suitable conditions on $V(x)$ are satisfied [8]:

$$P_\infty(x,v) = N \exp\left(-v^2/2KT - V(x)/KT\right). \tag{1.5}$$

Thus the late-time statistics of the velocity are Gaussian and uncorrelated with the position. It is notable that the stationary density has a closed tractable form for many nonlinear functions $f(x)$ when analytical study of the full evolution is not possible.

In this paper we examine how faithfully the stationary density is reproduced by standard timestepping methods for SDEs. These methods produce approximate values for position $X_n$ and velocity $V_n$ at discrete times $t_0, t_1, \ldots$, where $t_{n+1} - t_n = \Delta t$. We consider the evolution of $X_n$ and $V_n$, and their statistical properties as $t_n \to \infty$, and compare it with the exact form (1.4). In particular, we consider $P^*(y,u;t_n)$, the discrete-time analogue of (1.3), and compare the limit

$$P^*_\infty(y,u) = \lim_{t_n\to\infty} P^*(y,u;t_n),$$

where it exists, with $P_\infty(y,u)$. In this work we base our analysis on linear second-order equations, where the statistics are Gaussian and completely characterized by

three quantities: the mean squares of the position and velocity variables, and the correlation between the position and velocity.

The Euler and Heun methods simply treat (1.2) as a pair of SDEs, without attempting to take advantage of their special structure due to their origin in a single second-order differential equation. We shall show that they perform reasonably well at intermediate values of damping but fail at high damping, when the equations are stiff, and low damping, when it is important to conserve energy-like quantities over long times.

The Verlet algorithm [1, 9, 10] produces numerical solutions of second-order differential equations by updating the position variable without reference to the velocity variable. Extensions of this idea to Langevin equations [10, 11, 12, 13] have proved successful, and convergence properties may be analyzed using second-order difference equations [12, 14, 15]. The implicit midpoint rule cannot be written as a difference equation but can be written as a matrix equation [15]. Schurz [16, 17] studied multidimensional Ornstein–Uhlenbeck processes and showed that the implicit midpoint rule possesses the correct stationary distribution. Time-dependent properties of numerical algorithms for the class of linear equations considered in this paper can be considered by means of a modified frequency [15] or by the method of modified equations [18].

Recent analysis by Mannella [19, 20] of the stationary distribution resulting from numerical timestepping methods, based on an expansion of the exponent in (1.5), has led to a proposed modification of the leapfrog method. We shall take this method as one of our examples and find that it provides a notable improvement on the standard leapfrog method.

A slightly different system has been studied by Strømmen Melbø and Higham [21]. They considered a second-order system, but without a damping term. Rather than approaching a stationary density, the sum of the mean squared velocity and position grows proportional to time. Partitioned methods are superior to the Euler method for this system.

In section 2, we consider the case $f(x) = -gx$, where $g > 0$ is a constant, and $s(x) = 1$. That is, we consider linear second-order equations describing harmonic oscillators with additive white noise and damping. The statistics for linear systems are Gaussian, described by a covariance matrix, and can be calculated exactly in the continuous-time and discrete-time cases. A matrix equation is derived for the stationary variances and correlations resulting from a large class of numerical methods. We then calculate the stationary variances produced by some well-known methods. All methods we shall consider use one realization per timestep of a Gaussian distribution with mean zero and variance $\Delta t$. This framework includes many methods with multiple intermediate steps and implicit methods (which are in fact explicit for linear equations).

In section 3 we seek "measure-exact" methods for linear second-order SDEs, that is, methods that give the correct late-time mean square of the position and velocity and absence of correlation between them. In section 4, we restrict our consideration to Runge–Kutta methods for systems of additive noise SDEs and show that the unique measure-exact method is the implicit midpoint rule. In section 5 we report on numerical experiments carried out with $f(x) = x - x^3$ and $s(x) = 1$; in section 6 we report on numerical experiments carried out with $f(x) = x - x^3$ and $s(x) = x$. In both cases, of additive and of multiplicative noise in the double-well system, the implicit midpoint rule is the most satisfactory, with no error in two of the three quantities of

interest over the full range of values of damping. However, leapfrog methods have the benefit of being fully explicit.

**2. Linear equation and matrix notation.** If $f(x) = -gx$, then the stationary density (1.4) is

$$P_\infty(x, v) = N \exp\left(-g\, x^2/2KT - v^2/2KT\right).$$

The distributions of the position and velocity variables are Gaussian with

$$\lim_{t\to\infty} \left\langle \mathbf{X}_t{}^2 \right\rangle = \frac{1}{g} KT\ , \qquad \lim_{t\to\infty} \left\langle \mathbf{V}_t^2 \right\rangle = KT, \qquad \text{and} \qquad \lim_{t\to\infty} \left\langle \mathbf{X}_t \mathbf{V}_t \right\rangle = 0. \tag{2.1}$$

If $f(x) = -gx$ and $s(x) = 1$, then the linear second-order SDE can be written in matrix notation as

$$\mathrm{d}\begin{pmatrix} \mathbf{X}_t \\ \mathbf{V}_t \end{pmatrix} = Q \begin{pmatrix} \mathbf{X}_t \\ \mathbf{V}_t \end{pmatrix} \mathrm{d}t + \epsilon \begin{pmatrix} 0 \\ 1 \end{pmatrix} \mathrm{d}\mathbf{W}_t, \tag{2.2}$$

where

$$Q = \begin{pmatrix} 0 & 1 \\ -g & -\eta \end{pmatrix}. \tag{2.3}$$

We consider numerical updates for the linear system (2.2) that can be summarized as

$$\begin{pmatrix} X_{n+1} \\ V_{n+1} \end{pmatrix} = R \begin{pmatrix} X_n \\ V_n \end{pmatrix} + \epsilon r \Delta W_n, \tag{2.4}$$

where

$$R = \begin{pmatrix} r_{11} & r_{12} \\ r_{21} & r_{22} \end{pmatrix}, \qquad r = \begin{pmatrix} r_1 \\ r_2 \end{pmatrix}$$

and $\Delta W_n$ is sampled from a Gaussian distribution with mean zero and variance $\Delta t$, independently of $\Delta W_m$ for $n \neq m$. Since the numerical update (2.4) is a linear transformation, $P^*_\infty(x, v)$ is Gaussian. Let the correlation matrix be

$$\Sigma = \begin{pmatrix} \sigma_x^2 & \mu \\ \mu & \sigma_v^2 \end{pmatrix}, \tag{2.5}$$

where

$$\sigma_x^2 = \lim_{t_n\to\infty} \left\langle X_n^2 \right\rangle\ , \qquad \sigma_v^2 = \lim_{t_n\to\infty} \left\langle V_n^2 \right\rangle, \qquad \text{and} \qquad \mu = \lim_{t_n\to\infty} \left\langle X_n V_n \right\rangle.$$

Then

$$P^*_\infty(x, v) = \frac{1}{2\pi} |\Sigma^{-1}|^{\frac{1}{2}} \exp\left(-\frac{1}{2}(x, v)\Sigma^{-1} \begin{pmatrix} x \\ v \end{pmatrix}\right).$$

The stationary density $P^*_\infty(x, v)$ has the property of invariance under the transformation (2.4). Now, if $\binom{X_n}{V_n}$ is Gaussian with mean zero and correlation matrix $\Sigma$, then $R\binom{X_n}{V_n}$ is Gaussian with mean zero and correlation matrix $R\Sigma R^{\mathrm{T}}$. Thus the correlation

matrix that results from a method of the form (2.4) satisfies $\Sigma = R\Sigma R^{\mathrm{T}} + \epsilon^2 r r^{\mathrm{T}} \Delta t$, or

$$R\Sigma R^{\mathrm{T}} = \Sigma - \epsilon^2 r r^{\mathrm{T}} \Delta t. \tag{2.6}$$

In the remainder of this section, we shall use (2.6) to calculate the $\sigma_x^2$, $\mu$, and $\sigma_v^2$ as a function of $\eta$ and $\Delta t$ under six numerical methods for the case $s(x) = 1$. We can rewrite (2.6) in a form suitable for inversion:

$$\begin{pmatrix} r_{11}^2 - 1 & 2r_{11}r_{12} & r_{12}^2 \\ r_{11}r_{21} & r_{11}r_{22} + r_{12}r_{21} - 1 & r_{12}r_{22} \\ r_{21}^2 & 2r_{21}r_{22} & r_{22}^2 - 1 \end{pmatrix} \begin{pmatrix} \sigma_x^2 \\ \mu \\ \sigma_v^2 \end{pmatrix} = -\epsilon^2 \Delta t \begin{pmatrix} r_1^2 \\ r_1 r_2 \\ r_2^2 \end{pmatrix}.$$

The stability boundaries of the methods are functions of the parameters $\eta\Delta t$ and $g\Delta t^2$. Of the methods discussed below, the implicit midpoint rule and the leapfrog methods have the virtue of reducing to a symplectic method if $\eta = 0$ [5]. Further explicit methods with this property have been devised [6].

**2.1. Forward Euler method.** Under the Euler method, the position and velocity variables are updated as follows:

$$X_{n+1} = X_n + V_n \, \Delta t,$$

$$V_{n+1} = V_n - \eta V_n \Delta t + f(X_n) \, \Delta t + \epsilon \Delta W_n.$$

With the notation of (2.4), $R = R_{\mathrm{E}}$ and $r = r_{\mathrm{E}}$, where

$$R_{\mathrm{E}} = 1 + \Delta t Q = \begin{pmatrix} 1 & \Delta t \\ -g\Delta t & 1 - \eta \Delta t \end{pmatrix}, \tag{2.7}$$

$r_{\mathrm{E}} = \binom{0}{1}$ and the solution of (2.6) yields

$$\Sigma_{\mathrm{E}} = \frac{KT}{1 - \frac{g}{\eta}\Delta t} \left( 2 - \eta \Delta t + \frac{1}{2} g \Delta t^2 \right)^{-1} \begin{pmatrix} g^{-1}(2 - \eta\Delta t + g\Delta t^2) & -\Delta t \\ -\Delta t & 2 \end{pmatrix}. \tag{2.8}$$

In Figure 1 we display the differences between the stationary variances, obtained by applying the Euler method to the linear equation, and the exact values (2.1). The forward Euler method works best at intermediate values of $\eta$. It is unstable if $\eta\Delta t < g\Delta t^2$ or $\eta\Delta t > 2 + \frac{1}{2} g \Delta t^2$. In Figure 2, we plot the correlation between velocity and position, which is zero in the exact solution but is proportional to $\Delta t$ under the Euler method.

**2.2. The Heun method.** Under the Heun method, intermediate values are obtained via the Euler method:

$$\hat{X} = X_n + V_n \, \Delta t,$$

$$\hat{V} = V_n - \eta V_n \Delta t + f(X_n) \, \Delta t + \epsilon \, \Delta W_n.$$

The update is

$$X_{n+1} = X_n + \frac{1}{2}(V_n + \hat{V}) \, \Delta t,$$

$$V_{n+1} = V_n - \frac{1}{2}\eta(V_n + \hat{V})\Delta t + \frac{1}{2}(f(X_n) + f(\hat{X})) \, \Delta t + \epsilon \, \Delta W_n.$$

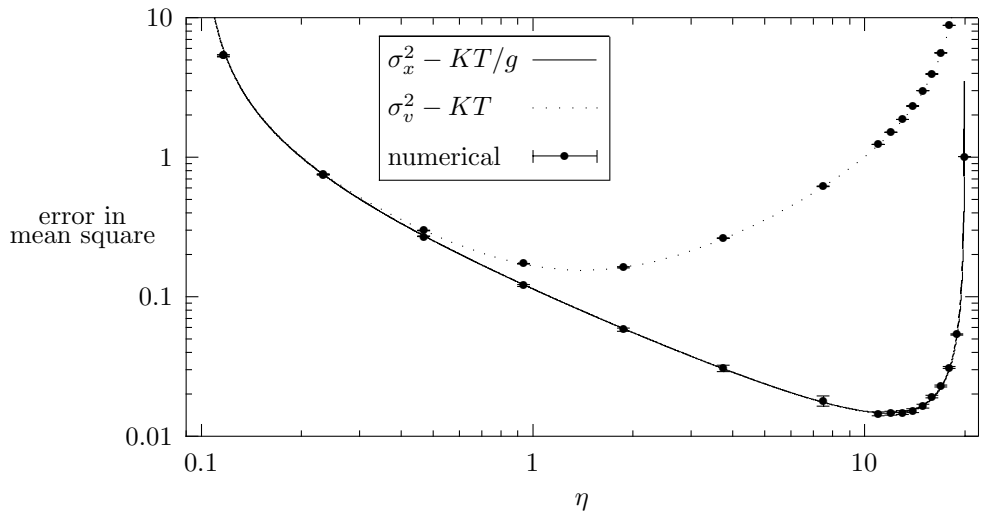


FIG. 1. *Mean squares versus damping for the forward Euler method. The differences between the late-time mean squares and the exact values are plotted against* $\eta$ *for fixed* $\Delta t = 0.1$, $g = 1$, *and* $KT = 1.0$. *The lines use* (2.8). *Dots with error bars are obtained from the numerical solution of the linear SDE.*

With the notation of (2.4), $R = R_{\mathrm{H}}$ and $r = r_{\mathrm{H}}$, where

$$R_{\mathrm{H}} = I + \Delta t Q + \frac{1}{2}\Delta t^2 Q^2 = \begin{pmatrix} 1 - \frac{1}{2}g\Delta t^2 & \Delta t - \frac{1}{2}\eta\Delta t^2 \\ -g\Delta t + \frac{1}{2}\eta g\Delta t^2 & 1 - \eta\Delta t + \frac{1}{2}(-g+\eta^2)\Delta t^2 \end{pmatrix}$$

and

$$r_{\mathrm{H}} = \begin{pmatrix} \frac{1}{2}\Delta t \\ 1 - \frac{1}{2}\eta\Delta t \end{pmatrix}.$$

Let $k_1 = \eta\Delta t$ and $k_2 = g\Delta t^2$. Then, for the stochastic Heun method,

(2.9)

$$\sigma_x^2 = \frac{KT}{g}\frac{1 - \frac{1}{4}k_1 + \frac{1}{8}k_1^2 - \frac{1}{32}(k_1k_2 + k_1^3) + \frac{3}{64}k_1^2k_2 - \frac{1}{32}k_1k_2^2 + \frac{1}{128}k_2^3}{\left(1 - \frac{1}{2}k_1 + \frac{1}{4}(k_1^2 - k_2) - \frac{1}{8}k_1k_2^2 + \frac{1}{16}k_2^2\right)\left(1 - \frac{1}{2}k_1 + \frac{1}{2}k_2 - \frac{1}{4}k_2^2/k_1\right)},$$

$$\sigma_v^2 = KT\frac{(1 - \frac{1}{2}k_2)^2}{\left(1 - \frac{1}{2}k_1 + \frac{1}{4}(k_1^2 - k_2) - \frac{1}{8}k_1k_2^2 + \frac{1}{16}k_2^2\right)\left(1 - \frac{1}{2}k_1 + \frac{1}{2}k_2 - \frac{1}{4}k_2^2/k_1\right)},$$

$$\mu = KT\Delta t\left(k_1 - \frac{1}{2}k_2\right)\frac{1 - \frac{1}{2}k_1}{\left(1 - \frac{1}{2}k_1 + \frac{1}{4}(k_1^2 - k_2) - \frac{1}{8}k_1k_2^2 + \frac{1}{16}k_2^2\right)\left(1 - \frac{1}{2}k_1 + \frac{1}{2}k_2 - \frac{1}{4}k_2^2/k_1\right)}.$$

Compared with the Euler method, the upper limit on $\eta$ for stability is little changed. The lower limit is, however, proportional to $\Delta t^3$. As $\Delta t \to 0$, the Heun method is stable if $(\frac{1}{2}g\Delta t^2)^2 < \eta\Delta t < 2$, and the correlation between position and velocity is proportional to $\Delta t^2$. See Figure 3.

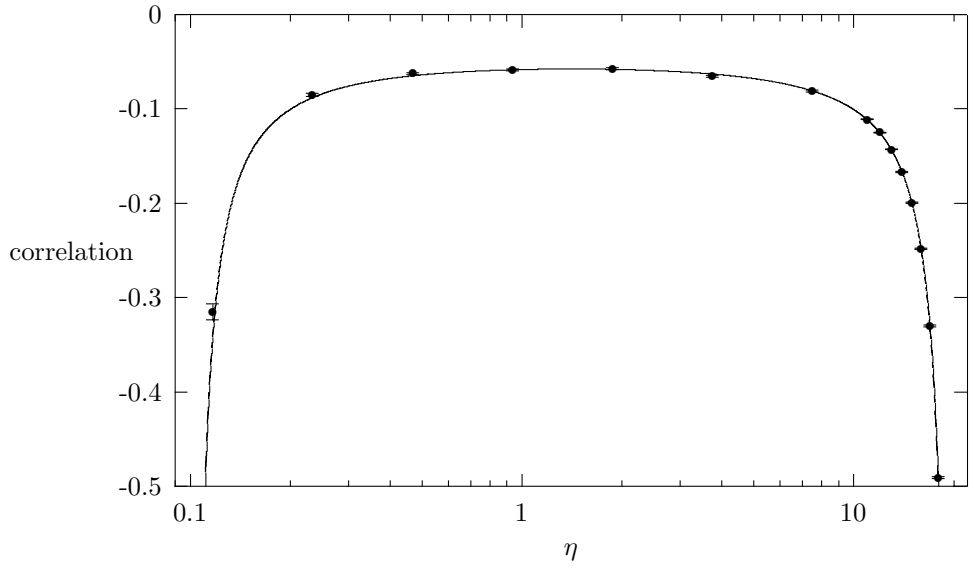


FIG. 2. *Position-velocity correlation versus damping for the forward Euler method. The late-time correlation, $\mu$, obtained using the forward Euler method, is plotted against $\eta$ for fixed $\Delta t = 0.1$, $g = 1$, and $KT = 1.0$. The line uses* (2.8). *Dots with error bars are obtained from the numerical solution of the linear SDE.*

**2.3. The leapfrog method.** Under leapfrog methods, velocity and position are updated successively rather than together. The simplest possible method is

$$\hat{X} = X_n + \frac{1}{2}V_n\Delta t,$$

$$V_{n+1} = V_n - \eta V_n \Delta t + f(\hat{X})\,\Delta t + \epsilon\,\Delta W_n,$$

$$X_{n+1} = \hat{X} + \frac{1}{2}V_{n+1}\Delta t. \tag{2.10}$$

Under this method, with the notation of (2.4), $R = R_{\mathrm{le}}$ and $r = r_{\mathrm{le}}$, where

$$R_{\mathrm{le}} = \begin{pmatrix} 1 - \frac{1}{2}g\Delta t^2 & \Delta t - \frac{1}{2}\eta\Delta t^2 - \frac{1}{4}g\Delta t^3 \\ -g\Delta t & 1 - \eta\Delta t - \frac{1}{2}g\Delta t^2 \end{pmatrix}$$

and

$$r_{\mathrm{le}} = \begin{pmatrix} \frac{1}{2}\Delta t \\ 1 \end{pmatrix}.$$

The leapfrog method maintains the independence of position and velocity and produces the exact stationary variance of the position variable. However, the error in $\sigma_v^2$ is an increasing function of $\eta$:

$$\Sigma_{\mathrm{le}} = KT \begin{pmatrix} g^{-1} & 0 \\ 0 & (1 - \frac{1}{2}\eta\Delta t - \frac{1}{4}g\Delta t^2)^{-1} \end{pmatrix}. \tag{2.11}$$

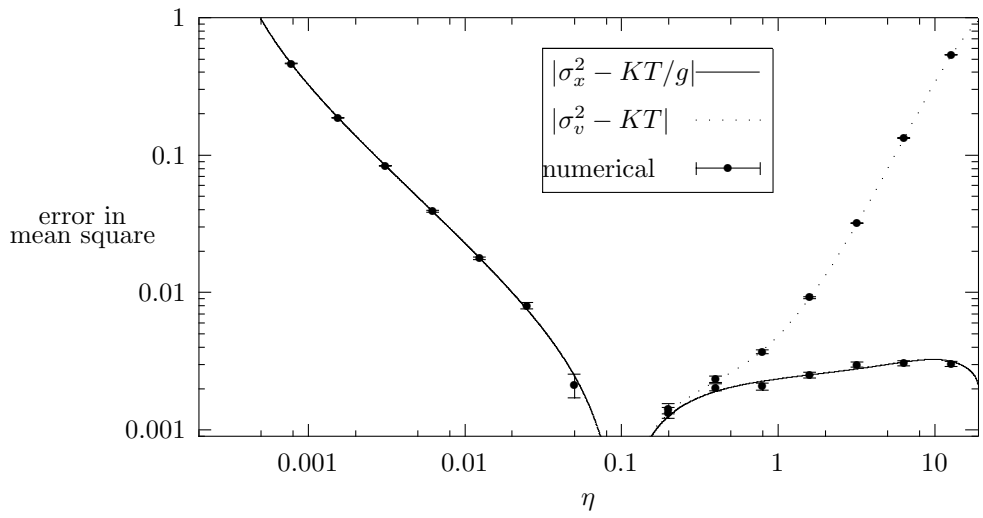


FIG. 3. *Mean squares versus damping for the Heun method. The differences between the late-time mean squares and the exact values are plotted against* $\eta$ *for fixed* $\Delta t = 0.1$, $g = 1$, *and* $KT = 1.0$. *The lines use* (2.9). *Dots with error bars are obtained from the numerical solution of the linear SDE.*

Mannella [19, 20] has proposed the following modification of the leapfrog method:

$$\hat{X} = X_n + \frac{1}{2}V_n\Delta t,$$

$$V_{n+1} = c_2\left(c_1V_n + f(\hat{X})\,\Delta t + \epsilon\,\Delta W_n\right),$$

$$X_{n+1} = \hat{X} + \frac{1}{2}V_{n+1}\Delta t,$$

where $c_1 = 1 - \frac{1}{2}\eta\Delta t$ and $c_2 = (1 + \frac{1}{2}\eta\Delta t)^{-1}$. The corresponding quantities are

$$R_{\mathrm{M}} = \begin{pmatrix} 1 - c_2\frac{1}{2}g\Delta t^2 & \frac{1}{2}\Delta t\left(1 + c_1c_2 - \frac{1}{2}c_2\Delta t^2\right) \\ -c_2g\Delta t & c_1c_2 - \frac{1}{2}c_2g\Delta t^2 \end{pmatrix},$$

$$r_{\mathrm{M}} = c_2\begin{pmatrix} \frac{1}{2}\Delta t \\ 1 \end{pmatrix},$$

and

$$\Sigma_{\mathrm{M}} = KT\begin{pmatrix} g^{-1} & 0 \\ 0 & (1 - \frac{1}{4}g\Delta t^2)^{-1} \end{pmatrix}. \tag{2.12}$$

The only error, in $\sigma_v^2$, is independent of $\eta$.

**2.4. The BBK method.** Under the Brünger–Brooks–Karplus (BBK) method [11], the position variable is updated without reference to the velocity variable. The

two most recent values of the position variable need to be retained, and the update is

$$X_{n+1} = X_n + \frac{1-\frac{1}{2}\eta\Delta t}{1+\frac{1}{2}\eta\Delta t}(X_n - X_{n-1}) + \frac{\Delta t}{1+\frac{1}{2}\eta\Delta t}\left(f(X_n) + \epsilon\,\Delta W_n\right).$$

With the definition of velocity $V_n\Delta t = X_n - X_{n-1}$, proposed in [12], the BBK method can be written in the form (2.4) with [22]

$$R_{\mathrm{B}} = \begin{pmatrix} 1 - \frac{g\Delta t^2}{1+\frac{1}{2}\eta\Delta t} & \frac{1-\frac{1}{2}\eta\Delta t}{1+\frac{1}{2}\eta\Delta t}\Delta t \\ -\frac{g\Delta t}{1+\frac{1}{2}\eta\Delta t} & \frac{1-\frac{1}{2}\eta\Delta t}{1+\frac{1}{2}\eta\Delta t} \end{pmatrix}$$

and

$$r_{\mathrm{B}} = \frac{1}{1+\frac{1}{2}\eta\Delta t}\begin{pmatrix}\Delta t \\ 1\end{pmatrix}.$$

Whatever the definition of velocity, we find [12, 15, 18]

$$\sigma_x^2 = \frac{KT}{g}\frac{1}{1-\frac{1}{4}g\Delta t^2}. \tag{2.13}$$

However, $\sigma_v^2$ and $\mu$ do depend on the definition of velocity. Note that, with the velocity definition $2V_n\Delta t = X_{n+1} - X_{n-1}$, the BBK update cannot be put into the form (2.4).

**2.5. The implicit midpoint method.** Under the implicit midpoint method, intermediate values are obtained via the implicit procedure

$$\hat{X} = X_n + \frac{1}{2}\hat{V}\,\Delta t,$$

$$\hat{V} = V_n - \frac{1}{2}\eta\hat{V}\Delta t + \frac{1}{2}f(\hat{X})\,\Delta t + \frac{1}{2}\epsilon\,\Delta W_n.$$

The update is

$$X_{n+1} = X_n + \hat{V}\,\Delta t,$$

$$V_{n+1} = V_n - \eta\hat{V}\Delta t + f(\hat{X})\,\Delta t + \epsilon\,\Delta W_n.$$

With the notation of (2.4), $R = R_{\mathrm{im}}$ and $r = r_{\mathrm{I}}$, where

$$R_{\mathrm{im}} = \left(I - \frac{1}{2}\Delta t Q\right)^{-1}\left(I + \frac{1}{2}\Delta t Q\right) = \begin{pmatrix} 1 - \frac{1}{2}\kappa^{-1}g\Delta t^2 & \kappa^{-1}\Delta t \\ -\kappa^{-1}g\Delta t & 2\kappa^{-1} - 1 \end{pmatrix},$$

and

$$r_{\mathrm{im}} = \kappa^{-1}\begin{pmatrix}\frac{1}{2}\Delta t \\ 1\end{pmatrix},$$

where $\kappa = 1 + \frac{1}{2}\eta\Delta t + \frac{1}{4}g\Delta t^2$. Thus

$$\Sigma_{\mathrm{im}} = KT\begin{pmatrix} g^{-1} & 0 \\ 0 & 1\end{pmatrix}. \tag{2.14}$$

Since $R_{\mathrm{im}}$ and $r_{\mathrm{im}}$ satisfy (2.6), the implicit midpoint method gives the exact stationary variances for all values of $\eta$. Only an algebraic error in Appendix A of [15] prevented this observation from being made by Mishra and Schlick. The behavior of the implicit midpoint method is explored further in section 4.

**3. Measure-exact algorithms.** We shall call a method "measure-exact" if its correlation matrix is the exact one for (2.2):

$$\Sigma_{\mathrm{e}} = KT \begin{pmatrix} g^{-1} & 0 \\ 0 & 1 \end{pmatrix}. \tag{3.1}$$

The $R$ and $r$ matrices for a measure-exact method satisfy (2.6) with $\Sigma = \Sigma_e$, that is,

$$R \begin{pmatrix} g^{-1} & 0 \\ 0 & 1 \end{pmatrix} R^{\mathrm{T}} = \begin{pmatrix} g^{-1} & 0 \\ 0 & 1 \end{pmatrix} - 2\eta r r^{\mathrm{T}} \Delta t. \tag{3.2}$$

We shall assume $\Sigma$ is positive definite and let $\Delta t$ be chosen small enough to ensure $G = \Sigma - \epsilon^2 r r^{\mathrm{T}} \Delta t$ is also positive definite. Matrices $\Sigma^{\frac{1}{2}}$ and $G^{\frac{1}{2}}$ can be constructed to satisfy $G = G^{\frac{1}{2}}(G^{\frac{1}{2}})^{\mathrm{T}}$ and $\Sigma = \Sigma^{\frac{1}{2}}(\Sigma^{\frac{1}{2}})^{\mathrm{T}}$. Let $\Sigma^{-\frac{1}{2}}$ and $G^{-\frac{1}{2}}$ be the inverses of $\Sigma^{\frac{1}{2}}$ and $G^{\frac{1}{2}}$. Condition (2.6) can then be rewritten as $PP^{\mathrm{T}} = I$, where $P = G^{-\frac{1}{2}} R \Sigma^{\frac{1}{2}}$ and $I$ is the identity matrix. Any $2 \times 2$ orthogonal matrix $P$ generates a solution of (3.2) as

$$R = G^{\frac{1}{2}} P \Sigma^{-\frac{1}{2}}. \tag{3.3}$$

A real $2 \times 2$ orthogonal matrix can be written as

$$P = \begin{pmatrix} (1-a^2)^{1/2} & a \\ -a & (1-a^2)^{1/2} \end{pmatrix},$$

for some $|a| \leq 1$. This form is convenient because we can take $a \propto \Delta t$, so that $P$ reduces to the identity matrix when $a = 0$.

With $\Sigma$ given by (3.1), we can choose

$$\Sigma^{\frac{1}{2}} = (KT)^{1/2} \begin{pmatrix} g^{-1/2} & 0 \\ 0 & 1 \end{pmatrix}.$$

So

$$G = \Sigma - r r^{\mathrm{T}} \Delta t = \begin{pmatrix} KT/g - r_1^2 \Delta t & -r_1 r_2 \Delta t \\ -r_1 r_2 \Delta t & KT - r_2^2 \Delta t \end{pmatrix},$$

and

$$G^{\frac{1}{2}} = \begin{pmatrix} \left(KT/g - r_1^2 \Delta t\right)^{\frac{1}{2}} & 0 \\ \frac{-r_1 r_2 \Delta t}{\left(KT/g - r_1^2 \Delta t\right)^{\frac{1}{2}}} & \left(KT - r_2^2 \Delta t + \frac{(r_1 r_2 \Delta t)^2}{KT/g - r_1^2 \Delta t}\right)^{\frac{1}{2}} \end{pmatrix}.$$

Any measure-exact method, using one Gaussian random variable per timestep, can be obtained from (3.3) with some choice of $a$, $r_1$, and $r_2$. For example, we may obtain a measure-exact Euler-like method by choosing $r = \binom{0}{1}$. That is,

$$G^{1/2} = (KT)^{1/2} \begin{pmatrix} g^{-1/2} & 0 \\ 0 & (1 - 2\eta \Delta t)^{1/2} \end{pmatrix}$$

and

$$R = G^{1/2} P \, \Sigma^{-1/2} = \begin{pmatrix} (1-a^2)^{1/2} & a g^{-1/2} \\ -a g^{1/2} (1 - 2\eta \Delta t)^{1/2} & (1-a^2)^{1/2} (1 - 2\eta \Delta t)^{1/2} \end{pmatrix}.$$

The Euler method is obtained as $\Delta t \to 0$ if $a = g^{1/2}\Delta t$. Thus

$$R = \begin{pmatrix} (1 - g\Delta t^2)^{1/2} & \Delta t \\ -g\Delta t(1 - 2\eta\Delta t)^{1/2} & (1 - g\Delta t^2)^{1/2}(1 - 2\eta\Delta t)^{1/2} \end{pmatrix}. \tag{3.4}$$

Notice that the difference between (3.4) and (2.7) is proportional to $\Delta t^2$. This modified Euler method reproduces the *exact stationary density* as long as $2\eta\Delta t < 1$. As a next step, we may impose agreement of $R$ with $\exp(\Delta t Q)$ to order $\Delta t^2$:

$$R = I + \Delta t Q + \frac{1}{2}\Delta t^2 Q^2 + \cdots .$$

Then $a = g^{\frac{1}{2}}\Delta t - \frac{1}{2}g^{\frac{1}{2}}\eta\Delta t^2$, $r_1 = \frac{1}{2}\Delta t + \cdots$, and $r_2 = 1 - \eta\frac{1}{2}\Delta t + \cdots$. Methods constructed in this way will have a stationary density differing from the exact density by some power of $\Delta t$.

Having established that measure-exact numerical methods do exist, in the next section we return to the question of solving condition (3.2) exactly, this time in the context of Runge–Kutta methods.

**4. Runge–Kutta methods for additive noise.** From the point of view of general Runge–Kutta methods, the system of two SDEs (1.2) with $s(x) = 1$ is a special case of the $m$-dimensional additive noise SDE that can be written [23]

$$\mathrm{d}\mathbf{Y}_t = f(\mathbf{Y}_t)\mathrm{d}t + \epsilon H \mathrm{d}\mathbf{B}_t,$$

where $\mathbf{Y}_t$ and $\mathbf{B}_t$ are $m \times 1$ column vectors, the entries of $\mathbf{B}_t$ are independent Wiener processes, and $H$ is an $m \times m$ matrix with constant entries. Let the numerically generated approximations be denoted by column vectors $y_n$. Under an $s$-stage Runge–Kutta method, $y_{n+1}$ is obtained from $y_n$ as a weighted sum of $s$ evaluations of the function $f$ at intermediate values $Y_i$:

$$y_{n+1} = y_n + \sum_{j=1}^{s} b_j f(Y_j)\Delta t + \epsilon H \Delta B_n,$$

where $\sum_j b_j = 1$. The $m$ entries of $\Delta B_n$ are drawn independently from a Gaussian distribution with mean zero and variance $\Delta t$. The column vectors of intermediate values satisfy

$$Y_i = y_n + \sum_{j=1}^{s} a_{ij} f(Y_j)\Delta t + \epsilon c_i H \Delta B_n. \tag{4.1}$$

Runge–Kutta methods for the case $s(x) \neq 1$ also exist [23].

We apply this general formalism to the linear equation (2.2) with $m = 2$. We have

$$y_n = \begin{pmatrix} X_n \\ V_v \end{pmatrix}, \ f(y) = Qy, \text{ and } H = \begin{pmatrix} 0 & 0 \\ 0 & 1 \end{pmatrix}.$$

Let $Y = (Y_1, Y_2, \ldots, Y_s)^{\mathrm{T}}$, $c = (c_1, c_2, \ldots, c_s)^{\mathrm{T}}$, $e = (1, 1, \ldots, 1)^{\mathrm{T}}$ and $A$ be the $s \times s$ matrix whose entries are the $a_{ij}$ in (4.1). Then (4.1) can be written

$$Y_i = e \otimes y_n + A \otimes Q Y_i \Delta t + \epsilon c \otimes \begin{pmatrix} 0 \\ 1 \end{pmatrix} \Delta W_n.$$

If $b = (b_1, b_2, \ldots, b_s)^{\mathrm{T}}$ , we can write

$$\begin{aligned} y_{n+1} &= y_n + b^{\mathrm{T}} Y \otimes Q\Delta t + \epsilon \begin{pmatrix} 0 \\ 1 \end{pmatrix} \Delta W_n \\ &= y_n + b^{\mathrm{T}} \otimes Q\Delta t \left(I_s \otimes I_m - A \otimes Q\Delta t\right)^{-1} \left( e \otimes y_n + \epsilon c \otimes \begin{pmatrix} 0 \\ 1 \end{pmatrix} \Delta W_n \right) \\ &\qquad + \epsilon \begin{pmatrix} 0 \\ 1 \end{pmatrix} \Delta W_n \\ &= \left( I_m + b^{\mathrm{T}} \otimes Q\Delta t \left(I_s \otimes I_m - A \otimes Q\Delta t\right)^{-1} e \right) y_n \\ &\qquad + \epsilon \left( I_m + b^{\mathrm{T}} \otimes Q\Delta t \left(I_s \otimes I_m - A \otimes Q\Delta t\right)^{-1} c \right) \begin{pmatrix} 0 \\ 1 \end{pmatrix} \Delta W_n. \end{aligned}$$

Thus

$$y_{n+1} = R(\Delta t Q) y_n + R_1(\Delta t Q) \begin{pmatrix} 0 \\ 1 \end{pmatrix} \epsilon \Delta W_n,$$

where, for scalar $z$,

$$R(z) = 1 + b^{\mathrm{T}} z (I_s - Az)^{-1} e$$

and

$$R_1(z) = 1 + b^{\mathrm{T}} z (I_s - Az)^{-1} c.$$

In the notation of (2.4), $r = R_1 \binom{0}{1}$. For example, the Euler method has $R = \Delta t Q$ and $r^{\mathrm{T}} = \begin{pmatrix} 0 & 1 \end{pmatrix}$.

Let us now examine the condition for an exact stationary measure. We shall take $g = 1$, which can always be achieved by rescaling time, so

$$\Sigma_{\mathrm{e}} = KT \begin{pmatrix} 1 & 0 \\ 0 & 1 \end{pmatrix}.$$

The equation to be satisfied is now

$$RR^{\mathrm{T}} - I + 2\eta \Delta t R_1 \begin{pmatrix} 0 & 0 \\ 0 & 1 \end{pmatrix} R_1^{\mathrm{T}} = 0. \tag{4.2}$$

Let

$$R(\Delta t Q) = I + \sum_{i=1}^{\infty} \alpha_i (\Delta t Q)^i$$

and

$$R_1(\Delta t Q) = I + \sum_{i=1}^{\infty} \beta_i (\Delta t Q)^i.$$

Then (4.2) can be expanded in powers of $\Delta t$ as

$$\begin{aligned}
&\Delta t\left(\alpha_1(Q+Q^{\mathrm{T}})+2\eta\begin{pmatrix}0&0\\0&1\end{pmatrix}\right)\\
&+\Delta t^2\left(\alpha_1^2QQ^{\mathrm{T}}+\alpha_2(Q^2+(Q^{\mathrm{T}})^2)+2\eta\beta_1\left(Q\begin{pmatrix}0&0\\0&1\end{pmatrix}+\begin{pmatrix}0&0\\0&1\end{pmatrix}Q^{\mathrm{T}}\right)\right)\\
&+\Delta t^3\Bigg(\alpha_3(Q^3+(Q^{\mathrm{T}})^3)+\alpha_1\alpha_2(Q^2Q^{\mathrm{T}}+Q(Q^2)^{\mathrm{T}})\\
&\qquad+2\eta\left(\beta_2Q^2\begin{pmatrix}0&0\\0&1\end{pmatrix}+\beta_2\begin{pmatrix}0&0\\0&1\end{pmatrix}(Q^{\mathrm{T}})^2+\beta_1^2Q\begin{pmatrix}0&0\\0&1\end{pmatrix}Q^{\mathrm{T}}\right)\Bigg)+\cdots=0.
\end{aligned}$$

If this equation is to be satisfied for all $\Delta t$, then each coefficient in the expansion must be zero. It is easily shown that this can hold if and only if $\alpha_i=(\frac{1}{2})^{i-1}$ and $\beta_i=(\frac{1}{2})^i$. Thus the family of Runge–Kutta methods that gives the exact stationary density is characterized by

$$R(\Delta tQ)=\left(I-\frac{1}{2}\Delta tQ\right)^{-1}\left(I+\frac{1}{2}\Delta tQ\right) \tag{4.3}$$

and

$$R_1(\Delta tQ)=(\Delta tQ)^{-1}(R(\Delta tQ)-I).$$

Explicitly, with $Q$ given by (2.3),

$$r=R_1\begin{pmatrix}0\\1\end{pmatrix}=\Delta t^{-1}\begin{pmatrix}-r_{22}-\eta r_{12}+1\\r_{12}\end{pmatrix}.$$

While Runge–Kutta methods with more than one stage can be constructed that have the stability function given by (4.3), they all have a singular tableau matrix. *The unique Runge–Kutta method, with a nonsingular tableau matrix, extended with a single Gaussian random variable per timestep, that preserves the exact stationary density of the linear equation for all values of damping, is thus the implicit midpoint method.* The method also has the virtue of being symplectic in the limit $\eta\to 0$ [5]. For linear equations, the method is explicit.

In the case of (2.2), the implicit midpoint rule is implemented as follows. We first generate $\hat{X}$ and $\hat{V}$:

$$\hat{V}=\kappa^{-1}\left(V_n-gX_n\frac{1}{2}\Delta t+\frac{1}{2}\epsilon\,\Delta W_n\right) \tag{4.4}$$

$$\hat{X}=X_n+\hat{V}\,\frac{1}{2}\Delta t, \tag{4.5}$$

where $\kappa=1+\frac{1}{2}\eta\Delta t+\frac{1}{4}g\Delta t^2$. Then

$$X_{n+1}=X_n+\hat{V}\,\Delta t, \tag{4.6}$$

$$V_{n+1}=V_n-\eta\hat{V}\Delta t-g\hat{X}\,\Delta t+\epsilon\Delta W_n. \tag{4.7}$$

Steps (4.4)–(4.7) are carried out in the order given.

**5. Double-well system: Additive noise.** The good properties of the implicit midpoint and leapfrog methods applied to linear second-order SDEs prompt us to investigate their accuracy for nonlinear equations. In this section we take as our example system (1.2), with the double-well potential

$$V(x) = -\frac{1}{2}x^2 + \frac{1}{4}x^4 \tag{5.1}$$

and with $s(x) = 1$. The stationary density is given explicitly by (1.5). The statistics of the position variable are non-Gaussian, but the mean is zero and $\sigma_x^2$ can be evaluated to arbitrary accuracy by a numerical evaluation of an integral.

In general, using an implicit method on a nonlinear equation requires an iterative procedure at each timestep. However, the structure of second-order systems makes a very simple iteration possible. First, the intermediate value $\hat{X}$ is generated by fixed-point iteration with the starting value $\hat{X} = X_n$. This amounts to repeated evaluation of

$$\hat{X} = X_n + \left(1 + \frac{1}{2}\eta\Delta t\right)^{-1} \frac{1}{2}\Delta t \left(V_n + \frac{1}{2}\Delta t f(\hat{X}) + \frac{1}{2}\epsilon\Delta W_n\right). \tag{5.2}$$

The rest of the algorithm is explicit:

$$\hat{V} = \left(V_n + \frac{1}{2}f(\hat{X})\,\Delta t + \frac{1}{2}\epsilon\,\Delta W_n\right) \Big/ \left(1 + \frac{1}{2}\eta\Delta t\right),$$
$$X_{n+1} = X_n + \hat{V}\,\Delta t,$$
$$V_{n+1} = V_n - \eta\hat{V}\Delta t + f(\hat{X})\Delta t + \epsilon\Delta W_n.$$

In our numerical experiments with the double-well system we used six iterations of (5.2), which was not a large overhead, comparable to an explicit predictor-corrector approach. However, in larger systems, where evaluation of $f(x)$ is computationally expensive, the number of iterations needs to be considered along with $\Delta t$.

In Figure 4 we display results obtained at $KT = 0.1$, using the Heun, leapfrog, and implicit midpoint methods, as a function of $\eta$ for $\Delta t = 0.1$. The Heun method is seen to be poor both at large and small values of damping, while the leapfrog method is accurate for small damping but inaccurate in $\sigma_v^2$ at large values of damping. The implicit midpoint method produces the exact values of $\sigma_v^2$ and $\mu$ at all values of damping but has a nonzero error in $\sigma_x^2$. Results for Mannella's modification of the leapfrog method are not shown in Figure 4 but are summarized as follows: the errors show little or no dependence on $\eta$, the error in $\sigma_x^2$ is comparable to that of the implicit midpoint method, while the error in $\sigma_v^2$ is similar to that of the standard leapfrog method as $\eta \to 0$.

In Figure 5 we display results obtained using the Heun and implicit midpoint methods, the standard leapfrog method, and Mannella's modified leapfrog method as a function of $\Delta t$, with $\eta = 1$ and $KT = 0.1$. Both leapfrog methods and the implicit midpoint method maintain the independence of position and velocity for all values of $\Delta t$. The implicit midpoint method also gives the exact value of the late-time mean square of the velocity variable. Mannella's modification of the leapfrog method leads to a reduced error in $\sigma_v^2$.

It is appropriate to compare numerical methods in a way that reflects their demand for computer resources. Figure 6 plots the errors in $\sigma_x^2$ and $\sigma_v^2$ as a function of

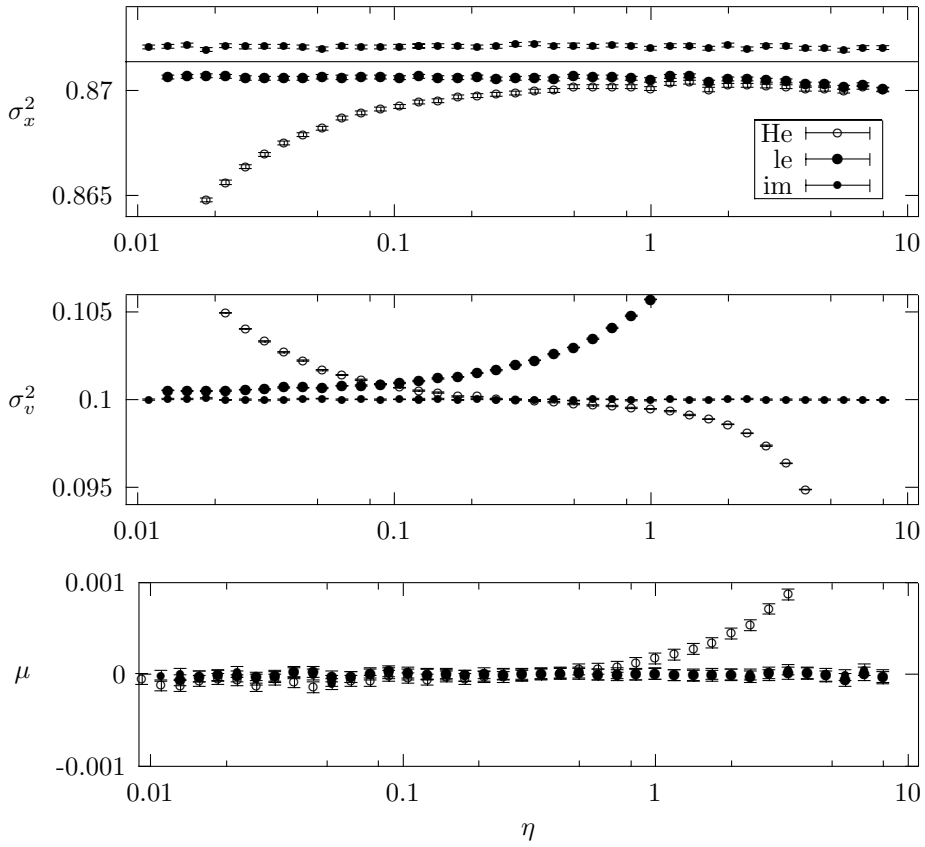


FIG. 4. *Mean squares and correlation versus damping: double-well system. Results obtained at* $KT = 0.1$ *using the Heun (circles), leapfrog (larger filled circles), and implicit midpoint (small filled circles) methods with* $\Delta t = 0.1$. *The top graph shows the late-time mean square of the position variable; the exact value is shown as a solid line. The middle graph shows the late-time mean square of the velocity variable; the exact value is* 0.1. *The lower graph shows the correlation between the position and velocity variables; the exact value is* 0.

the number of evaluations of $f(x)$ per time unit. In the cases of the leapfrog methods, the horizontal axis is simply $\Delta t^{-1}$. The Heun method requires two evaluations of $f(x)$ per timestep; the horizontal axis in this case is $2\Delta t^{-1}$. The implicit midpoint rule requires a total of eight such evaluations, six of them in the iterative step; the horizontal axis is thus $8\Delta t^{-1}$. All four methods have errors in $\sigma_x^2$ proportional to $\Delta t^2$; the extra computer time required for the iteration makes the implicit midpoint rule more expensive. On the other hand, the implicit midpoint rule reproduces the *exact* value of $\sigma_v^2$. Mannella's modification reduces the error in $\sigma_v^2$ associated with the leapfrog method.

**6. Double-well system: Multiplicative noise.** It is of interest to see how the methods analyzed and tested in this paper perform when extended to multiplicative noise systems, i.e., $s(x) \neq 1$. We first describe in the following steps how we have implemented them in our numerical experiments.

(i) Under the Heun method, intermediate values are obtained via the Euler

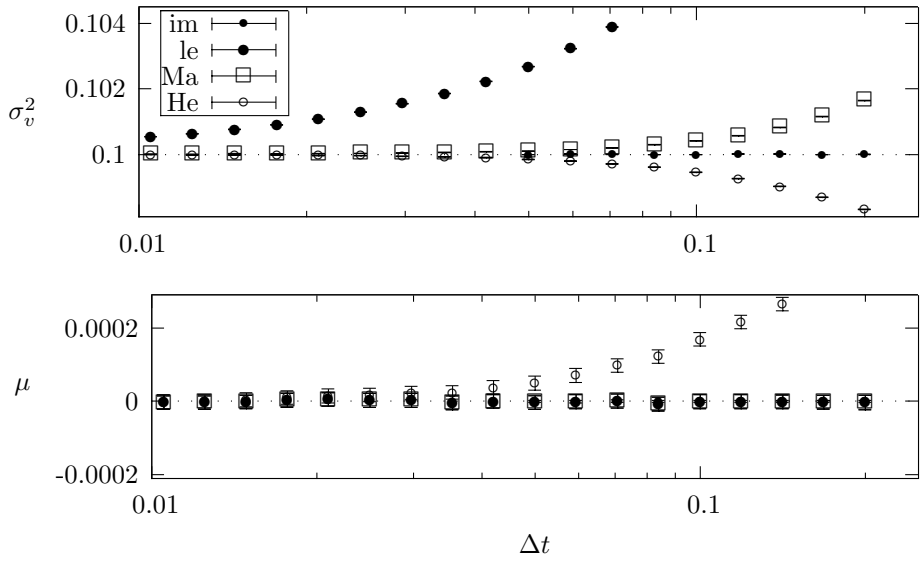


FIG. 5. *Mean-squared velocity and correlation versus $\Delta t$: double-well system. Results obtained at $KT = 0.1$ using the Heun method (circles), leapfrog method (larger filled circles), Mannella's modification (squares), and the implicit midpoint method (small filled circles) with $\eta = 1$. The top graph shows the late-time mean square of the velocity variable; the exact value is* 0.1. *The lower graph shows the correlation between the position and velocity variables.*

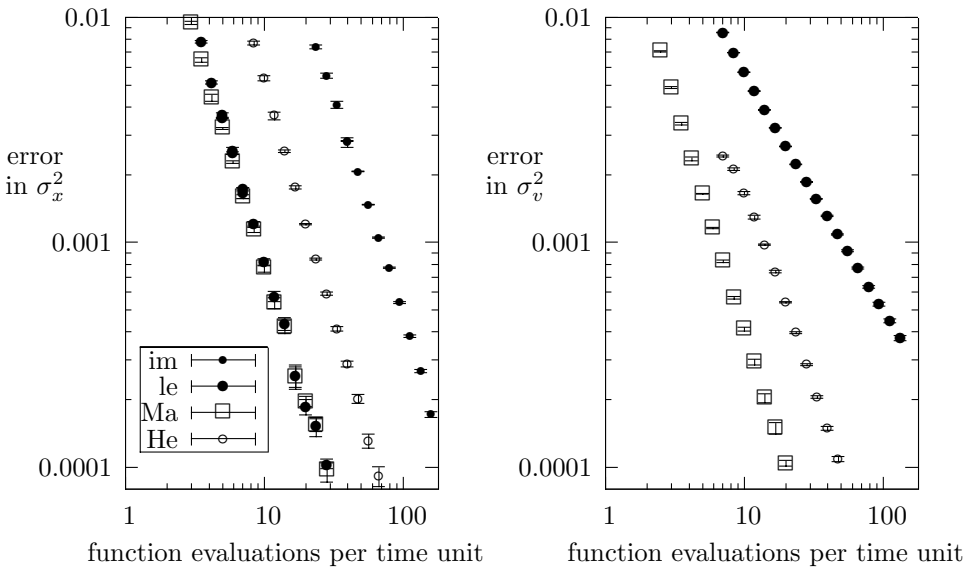


FIG. 6. *Error in mean squares: double-well system. Results obtained at $KT = 0.1$ and $\eta = 1$ using the Heun method (circles), leapfrog method (larger filled circles), Mannella's modification (squares), and the implicit midpoint method (small filled circles) with $\eta = 1$. The horizontal coordinate is $\Delta t^{-1}$ multiplied by the number of evaluations of $f(x)$ per timestep.*

method:

$$\hat{X} = X_n + V_n\,\Delta t,$$

$$\hat{V} = V_n - \eta s^2(X_n)V_n\Delta t + f(X_n)\,\Delta t + s(X_n)\epsilon\,\Delta W_n.$$

The update is

$$X_{n+1} = X_n + \frac{1}{2}(V_n + \hat{V})\,\Delta t,$$

$$V_{n+1} = V_n - \frac{1}{2}\eta(s^2(X_n)V_n + s^2(\hat{X})\hat{V})\Delta t + \frac{1}{2}(f(X_n) + f(\hat{X}))\,\Delta t + \frac{1}{2}\epsilon(s(X_n) + s(\hat{X}))\Delta W_n.$$

(ii) The standard leapfrog method is now

$$\hat{X} = X_n + \frac{1}{2}V_n\Delta t,$$

$$V_{n+1} = V_n - \eta s^2(\hat{X})V_n\Delta t + f(\hat{X})\,\Delta t + \epsilon s(\hat{X})\Delta W_n,$$

$$X_{n+1} = \hat{X} + \frac{1}{2}V_{n+1}\Delta t.$$

(iii) Mannella's leapfrog method is now

$$\hat{X} = X_n + \frac{1}{2}V_n\Delta t,$$

$$V_{n+1} = \left(1 + \frac{1}{2}s^2(\hat{X})\eta\Delta t\right)^{-1}\left(\left(1 - \frac{1}{2}s^2(\hat{X})\eta\Delta t\right)V_n + f(\hat{X})\,\Delta t + \epsilon s(\hat{X})\Delta W_n\right),$$

$$X_{n+1} = \hat{X} + \frac{1}{2}V_{n+1}\Delta t.$$

(iv) When using the implicit midpoint method, intermediate values $\hat{X}$ are generated by repeated evaluation of

$$\hat{X} = X_n + \left(1 + \frac{1}{2}s(\hat{X})^2\eta\Delta t\right)^{-1}\frac{1}{2}\Delta t\left(V_n + \frac{1}{2}\Delta t f(\hat{X}) + \frac{1}{2}\epsilon s(\hat{X})\Delta W_n\right),$$

with the starting value $\hat{X} = X_n$. The rest of the algorithm is explicit:

$$\begin{aligned}\hat{V} &= V_n + \frac{1}{2}\Delta t\hat{X},\\ X_{n+1} &= X_n + \hat{V}\,\Delta t,\\ V_{n+1} &= V_n - \eta s^2(X_{n+1})\hat{V}\Delta t + f(\hat{X})\Delta t + s(X_{n+1})\epsilon\Delta W_n.\end{aligned}$$

We have performed numerical experiments with $s(x) = x$. In Figure 7 we display results obtained at $KT = 0.1$, using the Heun method, Mannella's modification of the leapfrog method, and the implicit midpoint method, as a function of $\eta$ for $\Delta t = 0.1$.

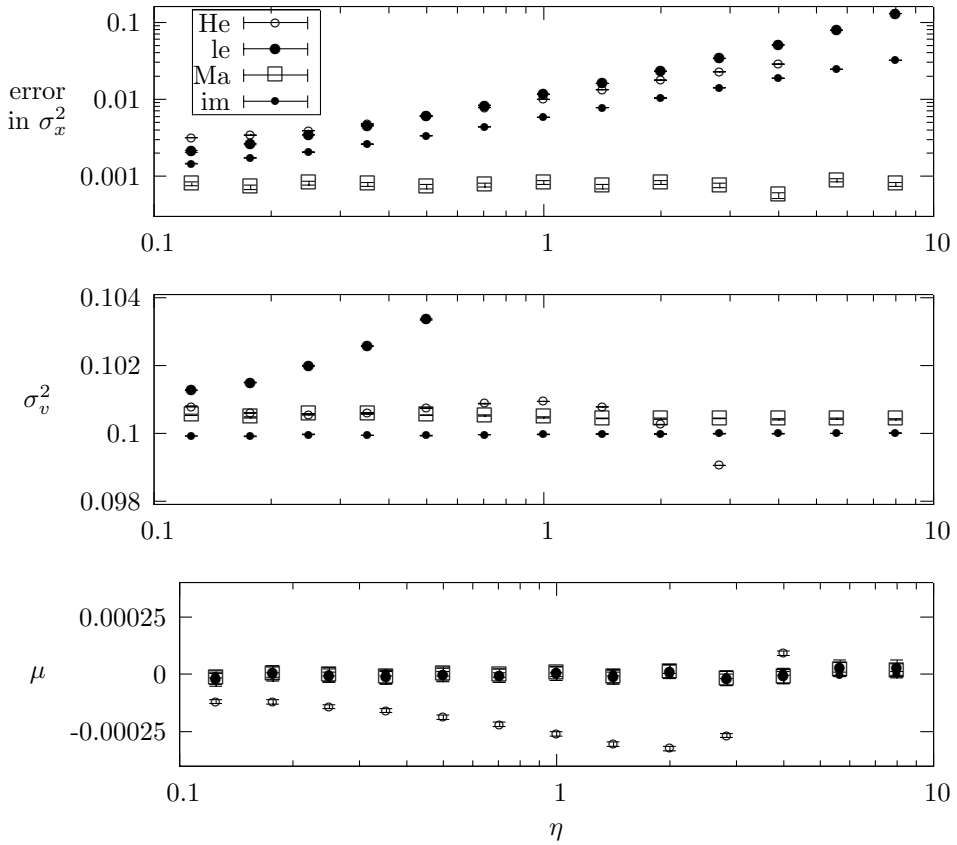


FIG. 7. *Mean squares and correlation versus damping: double-well system with multiplicative noise. Results obtained at* $KT = 0.1$ *and* $\Delta t = 0.1$ *using the Heun method (circles), the leapfrog method (larger filled circles), Mannella's modification of the leapfrog method (squares), and the implicit midpoint method (small filled circles). The top graph shows the error in the late-time mean square of the position variable (log scale). The middle graph shows the late-time mean square of the velocity variable; the exact value is* 0.1. *The lower graph shows the correlation between the position and velocity variables.*

In terms of the error in $\sigma_x^2$, Mannella's method performs best. The implicit midpoint method, however, is the only one that appears to give the exact value of $\sigma_v^2$ at all values of $\eta$. In Figure 8 we display numerical results with $KT = 0.1$ and $\eta = 1$ as a function of $\Delta t$. Mannella's method is the only one that has second-order convergence in $\sigma_x^2$, but the implicit midpoint method is more accurate in $\sigma_v^2$.

Note that, for systems of SDEs where there is a difference between Ito and Stratonovich forms, the implicit midpoint rule will converge to the Stratonovich form. However, it will only have strong order 0.5 for noncommutative SDEs with more than one noise term, in which case other approaches are needed to obtain a strong order of 1 [23, 24].

**7. Conclusion.** Exact calculations for linear equations are of interest in their own right and because the qualitative form of the error as a function of $\Delta t$ and $\eta$ carries over to the nonlinear equations used as examples here. The implicit midpoint rule is the only Runge–Kutta method with a nonsingular tableau matrix that reproduces

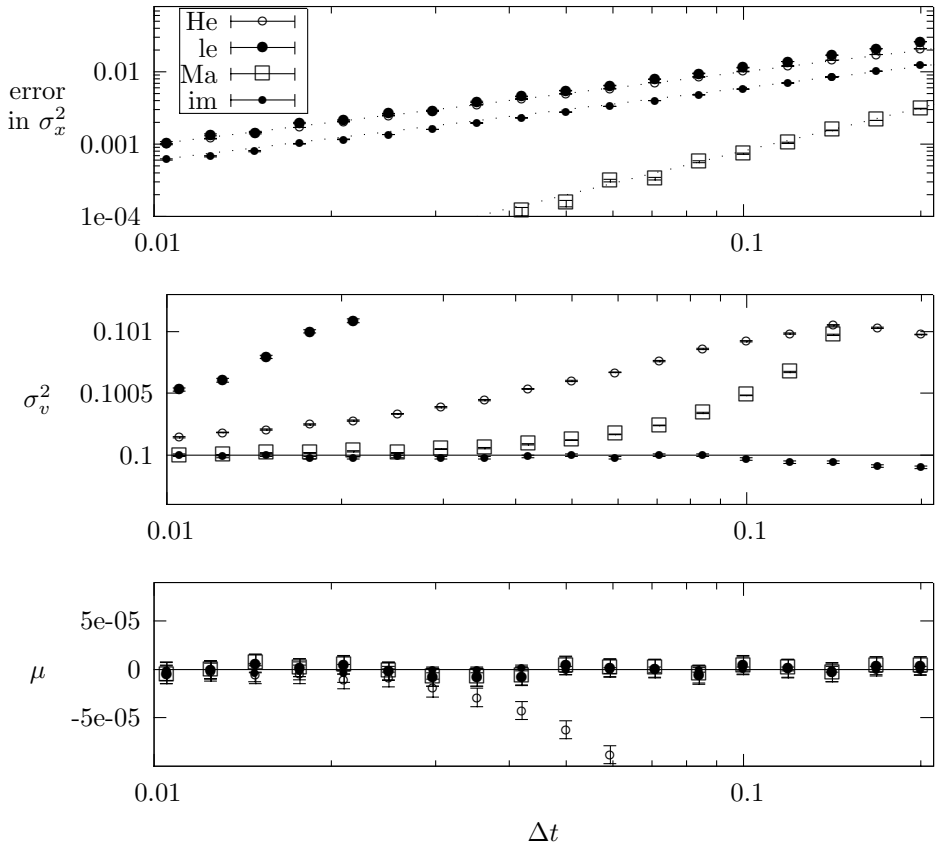


FIG. 8. *Mean squares and correlation versus $\Delta t$: double-well system with multiplicative noise. Results obtained at $KT = 0.1$ and $\eta = 1$ using the Heun method (circles), the leapfrog method (larger filled circles), Mannella's modification of the leapfrog method (squares), and the implicit midpoint method (small filled circles). The top graph shows the error in the late-time mean square of the position variable (log scale); the dotted lines are $0.1\Delta t$, $0.06\Delta t$, and $0.08\Delta t^2$. The middle graph shows the late-time mean square of the velocity variable; the exact value is 0.1. The lower graph shows the correlation between the position and velocity variables.*

the exact stationary distribution for all values of damping. It also performs well when applied to second-order nonlinear and multiplicative noise equations, with no apparent error in the stationary mean square of the velocity variable even for the nonlinear double-well system with multiplicative noise. However, leapfrog-type methods have the advantage of being fully explicit even for nonlinear equations. In particular, they require only one evaluation of the deterministic force per timestep.

Applied to linear equations, the simplest leapfrog method gives the exact stationary variance of the position variable and maintains the independence of position and velocity. Mannella's modification of the leapfrog method maintains this virtue while reducing the magnitude of the error in the variance of the velocity variable. We found similar qualitative behavior in our numerical experiments on the nonlinear double-well system: the implicit midpoint method and Mannella's method perform best, the former being superior in the error in $\sigma_v^2$ and the latter in $\sigma_x^2$.

In the deterministic case when solving separable Hamiltonian problems, explicit partitioned Runge–Kutta methods can be constructed that are symplectic. A chal-

lenge is to extend the idea in a stochastic setting to construct explicit partitioned methods that approximate the stationary correlation matrix with high-order accuracy.

**Acknowledgments.** GL thanks the Ethel Raybould Foundation and the Advanced Computational Modelling Centre of the University of Queensland for funding a visit in 2002. KB would like to thank the Australian Research Council for its funding of a Federation Fellowship.

## REFERENCES

[1] M. P. Allen and D. J. Tildesley, *Computer Simulation of Liquids*, Oxford University Press, Oxford, UK, 1997.
[2] C. A. Marsh and J. M. Yeomans, *Dissipative particle dynamics: The equilibrium for finite time steps*, Europhys. Lett., 37 (1997), pp. 511–516.
[3] T. Shardlow, *Splitting for dissipative particle dynamics*, SIAM J. Sci. Comput., 24 (2003), pp. 1267–1282.
[4] E. Hairer, S. P. Norsett, and G. Wanner, *Solving Ordinary Differential Equations* I: *Non-stiff Problems*, 2nd ed., Springer-Verlag, Berlin, 1993.
[5] E. Hairer, C. Lubich, and G. Wanner, *Geometric Numerical Integration: Structure-Preserving Algorithms for Ordinary Differential Equations*, Springer-Verlag, Berlin, 2002.
[6] G. N. Milstein and M. V. Tretyakov, *Quasi-symplectic methods for Langevin-type equations*, IMA J. Numer. Anal., 23 (2003), pp. 593–626.
[7] J. C. Mattingley, A. M. Stuart, and D. J. Higham, *Ergodicity for SDEs and approximations: Locally Lipschitz vector fields and degenerate noise*, Stochastic Process. Appl., 101 (2002), pp. 185–232.
[8] C. W. Gardiner, *Handbook of Stochastic Methods for Physics, Chemistry, and the Natural Sciences*, 3rd ed., Springer-Verlag, Berlin, 2004.
[9] L. Verlet, *Computer experiments on classical fluids.* I. *Thermodynamical properties of Lennard–Jones molecules*, Phys. Rev., 159 (1967), pp. 98–103.
[10] W. F. van Gunsteren and H. J. C. Berendsen, *Algorithms for Brownian dynamics*, Mol. Phys., 45 (1982), pp. 637–647.
[11] A. Brünger, C. L. Brooks III, and M. Karplus, *Stochastic boundary conditions for molecular dynamics simulations of st2 water*, Chem. Phys. Lett., 105 (1984), pp. 495–500.
[12] R. W. Pastor, B. P. Brooks, and A. Szabo, *An analysis of the accuracy of Langevin and molecular dynamics algorithms*, Mol. Phys., 65 (1988), pp. 1409–1419.
[13] J. A. Izaguirre and R. D. Skeel, *An impulse integrator for Langevin dynamics*, Mol. Phys., 100 (2002), pp. 3885–3891.
[14] G. Zhang and T. Schlick, *Implicit discretization schemes for Langevin dynamics*, Mol. Phys., 84 (1995), pp. 1077–1098.
[15] B. Mishra and T. Schlick, *The notion of error in Langevin dynamics.* I. *Linear analysis*, J. Chem. Phys., 105 (1996), pp. 299–318.
[16] H. Schurz, *The invariance of asymptotic laws of linear stochastic systems under discretization*, Z. Angew Math. Mech., 6 (1999), pp. 375–382.
[17] H. Schurz, *Preservation of probabilistic laws through Euler methods for Ornstein–Uhlenbeck processes*, Stochastic Anal. Appl., 17 (1999), pp. 463–486.
[18] W. Wang and R. D. Skeel, *Analysis of a few numerical integration methods for the Langevin equation*, Mol. Phys., 101 (2003), pp. 2149–2156.
[19] R. Mannella, *Quasisymplectic integrators for stochastic differential equations*, Phys. Rev. E, 69 (2004), 041107.
[20] R. Mannella, *Numerical stochastic integration for quasi-symplectic flows*, SIAM J. Sci. Comput., 27 (2006), pp. 2121–2139.
[21] A. H. Strømmen Melbø and D. J. Higham, *Numerical simulation of a linear oscillator with additive noise*, Appl. Numer. Math., 51 (2004), pp. 89–99.
[22] W. Wang, *Analysis of a Few Numerical Integration Methods for the Langevin Equation*, Master's thesis, University of Illinois at Urbana-Champaign, Urbana, IL, 2001.
[23] K. Burrage and P. M. Burrage, *Order conditions of stochastic Runge–Kutta methods by B-series*, SIAM J. Numer. Anal., 38 (2000), pp. 1626–1646.
[24] G. Lord, S. J. A. Malham, and A. Wiese, *Efficient strong integrators for stochastic linear systems*, submitted.